International Journal of Innovative Research in Engineering and Management (IJIREM)
ISSN (Online): 2350-0557, Volume-10, Issue-5, October 2023
https://doi.org/10.55524/ijirem.2023.10.5.11
Article ID IJIR2467, Pages 62-70
www.ijirem.org

A Suction-Powered Elastic-Strap Gripping Device

Er. Ishwar Singh[1], and Er. Janrdhan Kumar[2]

[1] M.Tech Scholar, Department of Mechanical Engineering, K.C. College of Engineering & Information Technology, Nawashahr, Punjab, India
[2] Assistant Professor, Department of Mechanical Engineering, K.C. College of Engineering & Information Technology, Nawashahr, Punjab, India

ABSTRACT- "In recent decades, there has been an increasing need for robotic gripping device capable of sensitively handling things of varied forms. While classic finger-shaped gripping devices are adaptable and can grab a broad variety of things, achieving a firm hold without slippage demands precise alignment of the fingers on the object. This study offers the notion of a ring-like delicate gripper that wraps across items much resembles an elastic string. The implied gripper is constructed of a flexible tube having layers of sponges interspersed with plastic sheets. By emptying the air inside the sponges, they contract, lowering the ring's diameter and permitting a tight grasp on things. This endows the gripper with the flexibility to wrap around items of varied forms flawlessly, leaving no opportunity for gaps. Moreover, the hardness of the compressed sponges inside the gripper mitigates any possible swaying of the grabbed items. Airborne particles inside The device that grips may be modified to fine-tune the grabbing energy. After air is emptied from the sponges, the gripper's minimal diameter is roughly one-fourth of its initial size. Consequently, our suggested gripper is set to find applications across a range of sectors, giving the potential to simply and firmly hold things while seamlessly adjusting to their various forms."

KEYWORDS- Soft Gripper, Robotic Handling, Object Manipulation, Gripping Technology, Flexible Automation

I. INTRODUCTION

The need for robotic grippers capable of independently manipulating things, especially fragile ones, has undergone a substantial growth in recent years. Traditional grippers, made with solid components and motors, confront substantial difficulty in firmly gripping delicate things like food without causing harm or slippage. This difficulty has sparked a rising interest in the subject of flexible robotics, typified by the utilization of malleable materials [1]-[2]. Numerous gripper designs using flexible appendages, modulated by internal air pressure, have been envisioned and brought to completion [3]–[6]. A select handful have even found their way into commercial applications [7]-[8]. Notably, there have been significant break through in the creation of flexible pneumatic grippers with the capacity to dynamically modify their stiffness [9]–[13]. However, grippers with finger-like designs demand precise control over finger motions and smart placement to prevent items from mistakenly passing between them.

In contrast to grippers equipped with fingers, different designs have been put forward. One such example is a universal gripper [14] that secures an item by deploying a flexible bag loaded with particles. The bag's stiffness is changed by changing the interior vacuum pressure, creating a stalling shift of the particulates [15]. In the example of the foldable charm sphere [16], a material is nestled within a cone-shaped grabber and wrapped by compressing the cone through differences in inner pressure from the vacuum. Notably, these gripping devices don't require flawless gripping for properly grabbing items. Nevertheless, the first case needs close touch with the object, which may not be suited for fragile goods. On the other hand, the latter is confined to items having circular cross-sectional forms. Consequently, we have created a novel gripper capable of firmly gripping items of varied forms without applying pressure. This peculiar circular in shape grabber [17], encompasses an item comparable to a stretchy strap by emptying the airborne particles inside. Even when presented with an item bearing a non-circular cross section, this gripper demonstrates amazing adaptation, adapting flawlessly to its surface.

Maintaining a good fit between the gripper and the item's surface is critical, since gaps may lower the contact area, thereby affecting the gripper's stability during object retention. Additionally, a smaller contact area leads to heightened contact pressure, which may result in the deformation of flexible items. Consequently, while handling products [18], like perishables or fragile objects, the gripper should deliver a light touch to guarantee a stable grasp.

A ground-breaking innovation is the vacuum-driven circular grabber [19]-[22], that was detailed in this paper. These feature a stiff cylinder in combination with a flexible rubber pack. Once filled with air that has been compressed, the bag conforms to an object

contained within the cylindrical structure. The cylindrical structure itself preserves its original form, perhaps restricting the capacity to visually check the gripping status of the encased object. Contrary to this, the gripping device generated in this study alters its shape to meet the object being handled. Consequently, the grabbing action is plainly viewable, making the gripper especially suitable for operations in constrained or tight places.
In this paper, we first sketch the layout of the gripper. Subsequently, we look into the experimental results concerning a telescopic actuator that has a similar internal arrangement with the aforementioned gripper. This actuator was created with the particular objective of improving the gripper's design. Following this, we explicate upon the technical capabilities of the designed gripper, encompassing its ability to deform features, capacity to encapsulate distinct items, and its grasping power. Lastly, we describe the process of affixing it to a robotic hand, along with its performance in handling a broad variety of things.

II. DESIGN OVERVIEW

We invented a unique technique exploiting the contracting capabilities of a sponge wrapped inside a bendable, airtight bag. Illustrated in Figure 1, we proposed a telescopic actuator adopting this idea. This actuator contained alternating layers of rectangular in shape spongy material and polypropylene strips (with a 0.15 mm thickness), all housed inside the sealed bag. Upon emptying the air from the pouch, the sponges experienced a contraction, resulting in the creation of recesses between the polypropylene layers, as indicated in Figure 1. Consequently, this contraction resulted to a decrease in the actuator's length along its longitudinal axis. The amount of this shortening changed in reaction to the internal vacuum pressure, as it was governed by the interaction between The pulling energy developed by the exerted force and the restorative energy of the sponges are used. Building upon this idea, we designed a gripper in the form of a ring that compresses whenever the internal airflow is expelled, as illustrated in Figure 2. As is explained in the next parts, this gripping device demonstrates exceptional flexibility, allowing it to wrap items of varied forms. Furthermore, the inner pressure of vacuum inside the gripping device may be adapted to fine-tune the clamping force. Upon restoration of the interior pressure of air to ambient levels, the sponges' intrinsic robustness reverts the grasping device to its normal form, thereby releasing the grabbed item.

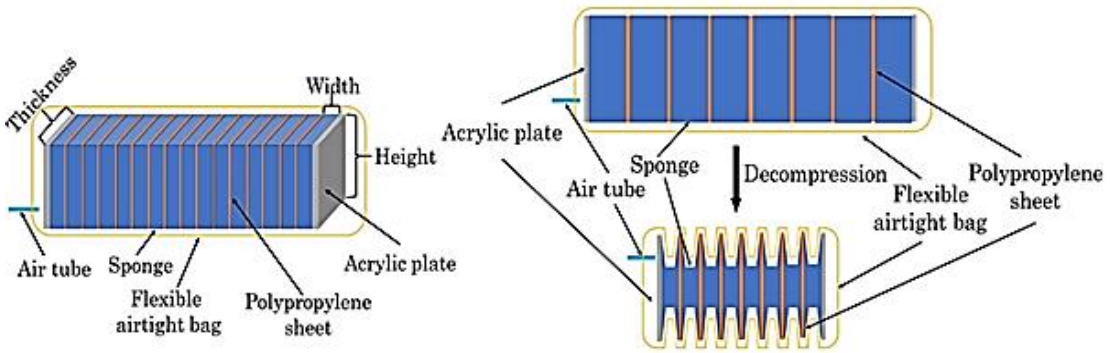

Figure 1: Portrays a Conceptual Representation of an Advanced Adjustable Actuating System

The above figure 1 portrays a conceptual representation of an advanced adjustable actuating system. This Device Comprises Rectangular Absorbent Material Arranged in an Alternating Pattern with PP Sheets, Enclosed within a Pliable, Airtight Enclosure. Upon Evacuating the Air Inside the Enclosure, the Absorbent Material Compress, Leading to a Reduction in the Actuating System's Length.

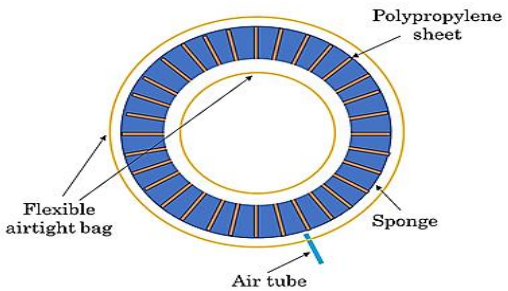

Figure 2: Presents a Schematic Overview of a Gripping Device. This Ingenious Tool Contracts and Encircles things of Enormous Designs within the Circular item by Expelling Air Particles via a Connected Conduit

A. Correlation Among Contraction Ratio of Telescopic Actuator And Spongy Material Shape

To maximize the gripper's adaptability in handling items of varied sizes, it's necessary to produce considerable shrinking of the gripper following air evacuation, notably impacted by the sponge's form. A important parameter for this augmentation is the maximum shrinkage ratio, indicating the reduction in the inner circumference of the ring compared to its starting condition. To streamline the internal design of the gripping device, our inquiry dug into the association among the form of the oblong box-like spongy material and the contraction ratio of the adjustable actuating system.

Fig. 1 depicts the specified dimensions of the sponge: width, height, and thickness. We concentrated our inquiry on the influence of sponge heights and widths on the contraction ratio across the actuator's longitudinal axis, keeping a constant thickness of 30 mm. We created samples of sponges in 15 unique sizes, varied in heights (31, 41, and 51 mm) and widths (11, 21, 31, 41, and 51 mm). Subsequently, we coupled three spongy material of each specification in a sequence, interposing PE strips, and wrapped them within an authentic rubberized casing, which had a thickness of 0.25 mm. The breadth of the sponge, showing the gap between polypropylene sheets, was gauged at an interior airborne pressure drop to -75 kPa.

Fig 3 indicates the correlation among the initial width of the spongy material and its contraction ratio at -75 kPa for different heights. It is found that when the breadth of the sponge decreases, the shrinkage ratio rises. Additionally, when the spongy material width is tiny, the vertical length has limited impact on the contraction ratio. Consequently, getting a larger contraction ratio for the actuator is attainable when the sponge width is below 10 mm. However, building a gripper with incredibly thin laminated sponges proved to be a tough undertaking. As a consequence, this research opts for sponges with a width of 10 mm in the gripper fabrication procedure to solve this problem.

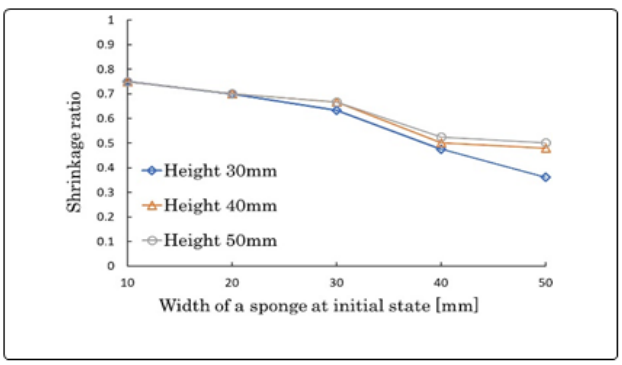

Figure 3: Illustrates the Correlation between the Absorbent Material's Initial Width and its Contraction Ratio

Figure 3 illustrates the Correlation between the Absorbent Material's Initial Width and its Contraction Ratio under an Internal Actuator Air Pressure of -75 KPA. The Compression Ratio was Diminished for Slimmer Absorbent Material. The Vertical Dimension of the Absorbent Materials had no Impact on the Compression Ratio when the Breadth of the Absorbent Material was Narrow

B. Correlation Among Extent of The Adjustable Actuating System And Interior Pressure of Air Particles

We made a research effort into the relation among the overall extent of the adjustable actuating system and its matching inner pressure of air. To create the actuator, we built a series of ten sponges, each measuring 31 mm in height, 31 mm in caliber, and 11 mm in breadth. These sponges were connected together using interlaced polypropylene strips and enclosed in an environmentally friendly rubber casing with an overall thickness of 0.25 mm. Instead of acrylic plates, we mounted hardwood pieces of similar dimensions (31 mm in height, 31 mm in caliber, and 13 mm in breadth) to both ends of the linked sponges, tying the actuating system to a gauging device.

In Fig 4, we illustrate the correlation among the actuator's extent (excluding the outside membrane and wooden components, notably the attached spongy material) and the interior pressure of air. Notably, the actuator suffered severe compression from ambient pressure to around -10 kPa, followed by a progressive contraction. Evacuating the air inside the actuator resulted in a curvature of the sponge ends, resulting to depressions among the polypropylene strips, as represented in Figure 1. These deformative and compressive features of the spongy material substantially impact the actuator's mechanism for shortening. This quick decrease in length under low vacuum pressure hence allows the gripping device to delicately grasp items, as described in the sections to come.

C. Contracting Coerce of The Adjustable Actuating System

The gripping device, behaving analogous to a rubber band, surrounds an item by the contracting coerces developed by reducing interior negative pressures. This contraction, upon surrounding the item, provides a wrapping coerce right angled to the surface area. To analyze this encapsulating coerce, we studied the association between the telescopic actuator's compression force and its length. Employing a global testing apparatus and a force gauge, we executed the subsequent method.

Initially, one side of the actuating system was fastened to the UTM's foundation, and the actuator's interior air pressure was calibrated to the desired value, effectuating its contraction. Subsequently, the another side of the compressed actuating system was fastened to the coerce gauge, paying particular

attention to its location to avoid any unnecessary stretching.

The compression coerce was then gauged subsequent to dropping the interior pressure of air to -75KPA. Furthermore measurements of compression forces were made for varied extents of the actuating system by altering interior pressures of air to 0, -4, -6, -11, -21, -31, -41, and -60 kPa. For each length of the actuator, three measurements were obtained, and the overall averages were determined. Given that the compression force derives from the discrepancy among the internal pressure of air and the pressure when fastened to the coerce gauge, it is claimed that the compression coerce is stronger when the actuating system's extent approximates its inherent condition as opposed to when it is compressed.

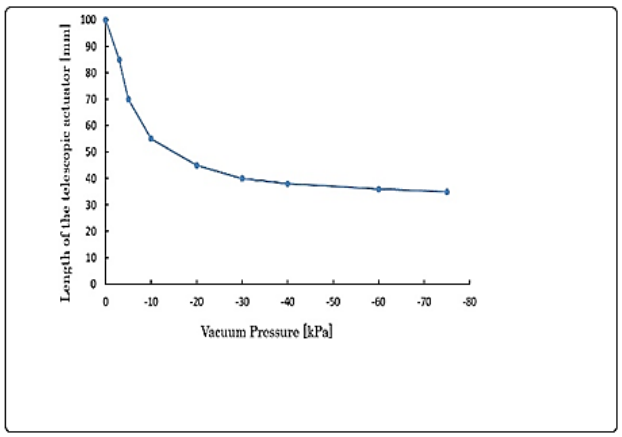

Figure 4: Illustrates the Correlation between the Adjustable Actuating System's Length and Internal Air Pressure

The above figure 4 illustrates the Correlation between the adjustable actuating system's length and internal air pressure. initially, at atmospheric pressure, the pressure, the actuator underwent substantial contraction, reaching a minimum at around -10 kpa. subsequently, it exhibited a gradual reduction in length.

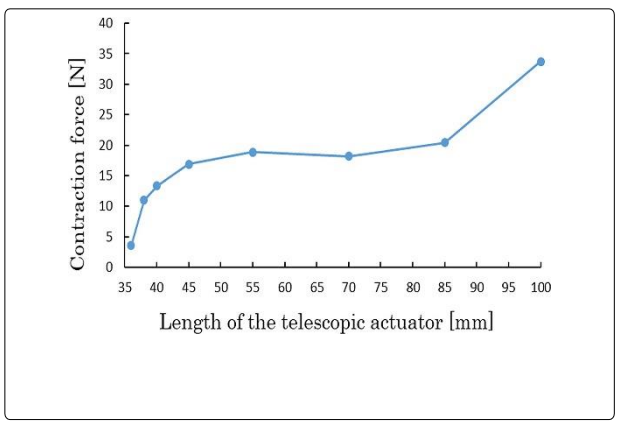

Figure 5: Illustrates the Correlation between the Extendable Actuator's Compression Strength

In figure 5 Illustrates the Correlation between the Extendable Actuator's Compression Strength under an Internal Atmospheric Pressure of -75 KPA and its Length. The Strength Remained Relatively Stable Within the 45-85 mm Range. This Constancy Arose from the Extender's Substantial Length Alteration between Ambient Pressure and Roughly -10 KPA. Within this Span, the Internal Pressure Exhibited Little Variation, Ensuring a Consistent Compressive Strength. Beyond 85 MM, a more Pronounced Incline was Observed, likely Attributable to Alterations in the Extender's Profile Area caused by Surface Dents.

Figure 5 depicts the association among the extent of the adjustable actuating system and the energy of compression. It was noticed that a smaller actuator length resulted in a lower contraction force, corresponding with the predicted consequence. The continuous compression force reported from 45 to 85 mm actuator extent was ascribed to the considerable shift in actuator length, which happened from ambient pressure to around -10 kPa. Within this spectrum, the change in interior pressure of air was negligible. Consequently, the compression force, which relies on the discrepancy between beginning pressure of air and vacuum pressure (i.e., about -75 kPa in this specific research), displayed minor fluctuation. The escalation in compression force with extent shift from 84 to 101 mm may be explained to modifications in profile area due to indentation of spongy material, as previously stated.

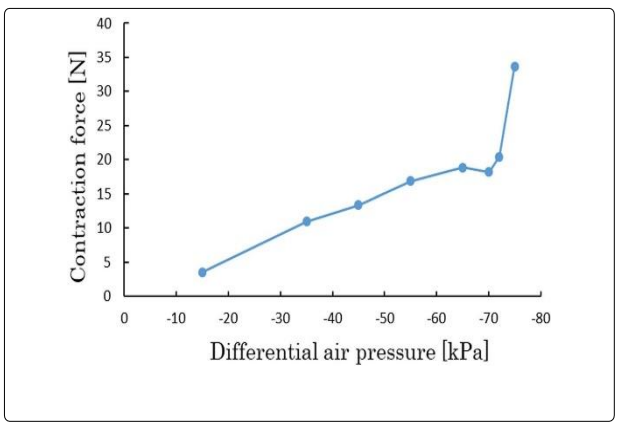

Figure 6: Connection between the Compressive Strength and the Distinction in Internal Atmospheric Pressure

In the above figure 6 depicts the Connection between the Compressive Strength and the Distinction in internal atmospheric pressure, particularly when the the manipulator is attached to the instrument in contrast to the pressure while taking quantification (-75 kPa). Significantly, the compressive strength demonstrated a near-linear relationship with the divergence in atmospheric pressure.

D. Substance of The Exterior Film for the Elastic-Strap Gripping Device

To optimize the contraction fraction (ratio) of the elastic-strap traction, it is recommended to apply an external barrier that delivers flexibility without restricting the shrinkage of the spongy material. In accordance with the beam theory, the degree of rigidity in bending is calculated by the multiplication of modulus of elasticity and the flexural rigidity. Hence, in order to opt for a match exterior film for the gripping band, three gripping devices were made, each including distinct exterior films of differing calibers and modulus of elasticity. Each of these gripping devices housed 50 spongy material, each having a height of 30 millimeters, a caliber of 20 millimeters, and a width of 10 mm. These sponges were securely glued together in a circular design using interlaced polypropylene sheets approximately 0.15 mm in thickness. The starting internal circumference of each gripping device was set at 149 mm.

Table 1 demonstrates the elements utilized for the exterior film within the gripping devices. The disclosed bending rigidity parameters in the table were determined in accordance with beam theory. A PVC film, lined with cotton, was selected as the film on the outside due to the potential of the unlined PVC film to undergo plastic deformation even at minor forces. The use of a cotton liner serves to enhance the Young's modulus and prevent deformation due to plasticity. The polyethylene tarpaulin utilized in the study comprised a basic pattern of polyethylene tape varied in width from 2 to 4 mm. It's worth mentioning that the flexural rigidity of the tarpaulin, as illustrated in Table 1, is similar to that of a PE sheet of exact caliber. Consequently, it is likely that the true bending rigidity of the poly trap may be significantly lower as opposed to figure.

Table 2 reveals the contraction fraction (ratio) determined after the internal of every gripping device was decompressed to −75 kPa. Among the materials evaluated the Poly VC-coated cotton fabric, demonstrating the greatest flexural rigidity, had the lowest contraction ratio. The poly tarp and latex revealed fairly identical shrinkage ratios. However, the grasping device utilizing the poly tarp demands a extended period to recover to its former shape once freed from airtight conditions. Conversely, the grasping device employing the naturally occurring rubber membrane rapidly recovered to its prior state. This shows that the toughness of the petroleum-based rubber membrane may expedite the expanding process of the grasping device. Consequently, we selected for the use of natural rubber as the membrane on the outside for the suggested gripping device.

Table 1**:** Caliber, Modulus of Elasticity, and Flexural Rigidity of every substance

Substance	**Caliber [mm]**	**Modulus of Elasticity [MPa]**	**Flexural Rigidity [Nm^2]**
PVC-coated cotton fabric	0.4	189	1.30×10^{-5}
Polyethylene Tarpaulin	0.08	406	3.5×10^{-7}
Natural Rubber	0.29	4	1.2×10^{-7}

Table 2**:** Correlation Among Outermost Membrane Substance and Contraction Ratio

Substance	**Contraction Ratio**
PVC-coated cotton fabric	0.7
Poly tarp	0.8
Latex	0.8

II. EXPERIMENTS

This section explains the encapsulating effectiveness of the gripping device having a rubber sheet, following by an elaboration of the procedure for affixing the instrument to an automated arm.

A. Correlation Among Inner Pressure of Air And the Inner Circumference of the Gripping Device

The investigation explored into the relationship between the inner circumference of the gripping device and its air pressure within it. The researchers collected measurements of the inner diameter as they meticulously altered the internal pressure. This was done in increments of 1 kPa from 0 to -10 kPa, followed by advances of 10 kPa from -10 to -70 kPa, and eventually at -75 kPa. As displayed in Figure 7, the gripper revealed distortions, while Figure 8 highlights the link among the pressure of the internal air and the associated contraction ratio. Notably, the gripper's contraction ratio displayed a rapid rise with the initial increase in vacuum pressure, reaching its peak at around -10 kPa, akin to the behavior reported in telescopic actuators. Subsequently, the expansion became more sluggish. Beyond vacuum pressures of -30 kPa, changes in the inner circumference were unambiguously modest.

B. Effectiveness of Surrounding An Item

The gripper's encasing effectiveness was evaluated with a variety of objects: an empty bottle with a circumference of 110 mm, typical triangular prisms in order with sides measuring 70 mm and 95 mm, a plate measuring 120 mm by 15 mm, a conical object

with a surface circumference of 105 millimeters & a side length of 75 millimeters, & a Cross like shape refractor composed of three refractors. As demonstrated in Fig 9, when the pressure inside the device was lowered to -75 kPa, the gripping device successfully gripped the container and platter without leaving spaces in between. While the gripping device managed to encase the triangle prisms, minor spaces emerged, especially for the smaller one.

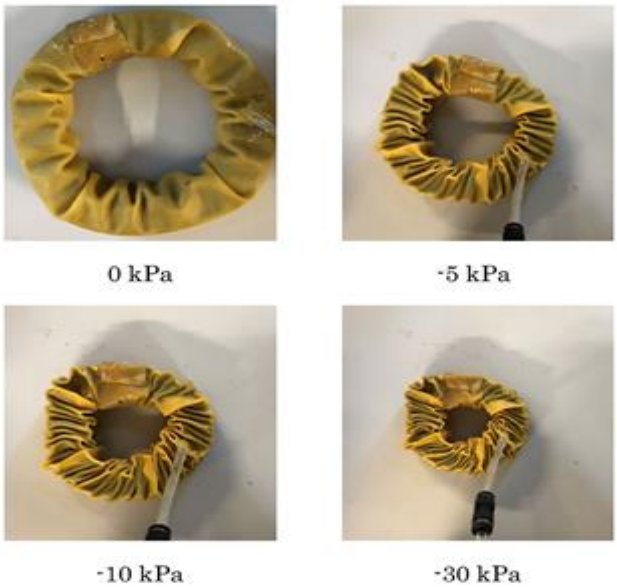

Figure 7: Demonstrates the Distortions Observed in an Elastic Loop Clasper under Varying Suction

In the above figure 7 demonstrates the distortions observed in an elastic loop clasper under varying suction levels (0, -5, -10, and -30 kPa). Remarkably, even at a relatively low negative pressure of -5 kPa, the clasper contracts significantly. As the suction level escalates to -30 kPa, the interior breadth of the clasper reaches its near-minimum point, showcasing a substantial reduction in size.

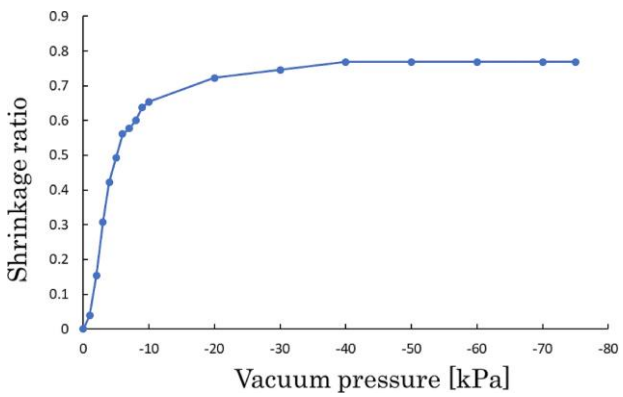

Figure 8: Depicts the relationship between the inner pneumatic force and contraction proportion of the internal gauge of an elastic loop holder

In figure 8 depicts the relationship between the inner pneumatic force and contraction proportion of the internal gauge of an elastic loop holder. The holder contracted rapidly when the within vacuum force decreased. The contraction proportion altered softly within negative atmospheric the pressure dropped below -10 kPa and then stabilized when the pneumatic force surpassed -30 Kpa

The gripping device adeptly wrapped across the plate with no any obvious flaws. Thus, it has been discovered that the appearance of spaces is not primarily driven by contour, but also influenced by the slants of the sides and the surrounding extent of the item. While an item comprises a very narrow peripheral length, encircling it becomes problematic, especially if it includes sharp edges. This problem originates from the constrained deformation capability of the gripper when it suffers compression preparatory to making contact with the object's surface.

In the instance of the cone, the gripper exhibited the capacity by encasing the sloping surface via a twisting action. To evaluate this capability, the gripping device was constricted, with its bottom portion making impression on the top half of a 100 mm circumference pillar, leaving a 5 mm gap. This wrapping process is portrayed in Figure 10. Notably, even after the bottom element of the gripping device reached the pillar, the top an element continued to compress, resulting in a 90° rotation of the gripper. The inner circumference of the gripping device, after this 90° twist, matched its smallest innermost circumference witnessed after compression without enclosing any objects, as illustrated in Figure 7. Consequently, when wrapping about a cone, the smallest angle of slope (θ) at which the gripping device can achieve interaction with the surface is contingent upon the bare minimum inner circumference of the gripping device (dmin) under vacuum conditions, the circumference of the cone with the lower part of the gripping device in contact (dc), & the elevation of the gripping device (h).

Figure 9: Execution of Clutching items of Enormous Forms

The above Figure 9 Execution of clutching items of enormous forms: a flask; b small three-sided column; c

large three-sided column; d platter; e funnel; f cruciform column. The clasp encircled the flask, platter, and funnel seamlessly. The clasp encircled the three-sided columns. However, more prominent openings were noted for the smaller three-sided column. With a funnel, the clasp contorts and envelops the incline. With a cruciform column, openings emerged in the hollowed regions.

C. Contact Pressure

The research probed into the association between the gripper's contact pressure and vacuum pressure utilizing a 100 mm diameter pillar as a test subject. To assess the contact pressure, AMI3037-SB-SET, air bladder pressure sensor from AMMI TECHNOLOGY, Inc., was used. Measurements were obtained while the interior pressure of air fluctuated from -20 to -80 kPa, in 10 kPa intervals. The point of contact pressure was obtained using three distinct measurements, afterwards averaged for accuracy. An escalation in internal vacuum pressure led to a proportionate rise in contact pressure. Given that the gripping action of the gripping device nears completion at a negative pressure below -30 kPa, as explained in the last part, boosting the negative pressure helps to improve the contact pressure. Conversely, ceasing air suction while the gripping device is in touch with an item has the effect of lowering the contact pressure. Assuming a constant contact area and uniform contact pressure, the encapsulating force (comprising the summation of pressure from contact over all contact places) corresponds directly with the contact pressure. Nonetheless, it's worth noting that this supposition could be incorrect for objects having non-circular cross-sectional profiles. Looking forward, the study's potential possibilities involve a research of the correlation among item form and impact force.

D. Deployment on the Automated Wrist

The layout of the setup for affixing the created gripping device onto a robotic arm is represented in Figure 11. Secured by fine cotton threads with a 1 mm diameter, the gripper and three links, each measuring 195 mm in length, are kept in place. Moreover, the links are connected to a metallic ring with a diameter of 110 mm, which is fastened to the robot arm. This configuration provides for a loose connection between the gripping device, connections, and metallic ring, acting comparable to a ball junction. Furthermore, the cords display flexibility, permitting unfettered movement of the connections without encumbering the gripper's deformation.

Figure 10 depicts the operational procedure employed by this equipment for lifting a selection of objects: a plastic bottle weighing 900 grams, a mug weighing 280 grams (with the gripper specifically targeting the handle), a toy duck weighing 65 grams, a book weighing 165 grams, a box weighing 134 grams, and a square bread

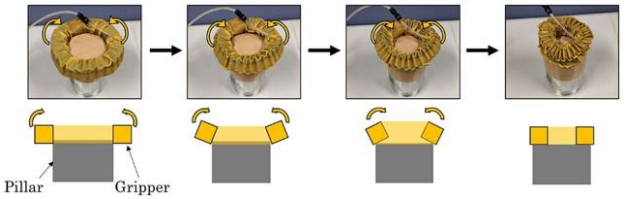

Figure 10: Illustrates the gripper's rotational movement upon making contact between its lower section and the upper surface of a pillar.As the gripper's internal air is removed, the upper portion undergoes further compression, resulting in a twisting action that persists until reaching a 90° angle.

loaf weighing 166 grams. The findings underline the adaptability of the gripper mounted to a robotic arm in manipulating items of varied forms. In the instance of the bread, air evacuation was ceased at -3 kPa to avoid any unnecessary compression of the delicate loaf when encased without any holes. This study indicates the gripper's capacity to secure a soft item with a non-circular cross-section, but needing careful adjustment of internal air pressure in line with the contact circumstances.

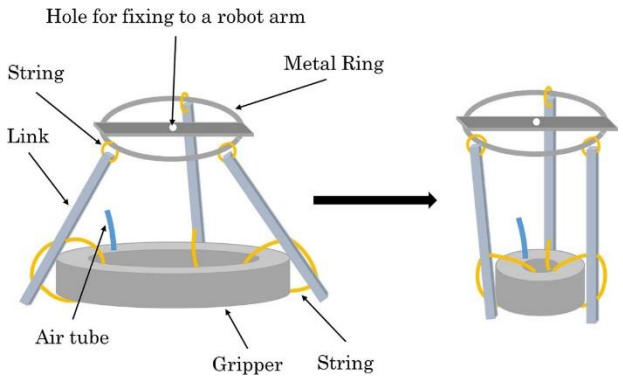

Figure 11: Graphical Depiction of the Clamping Mechanism

The above figure 11 Graphical Depiction of the Clamping Mechanism. The three links are linked with cords to the grabber and a metallic band for fastening to the arm of the robot. The cords are elastic so that the connections move easily without compromising with the distortion of the gripping device. The examination focused on identifying the maximum weight capacity of the gripper while handling different items. These comprised polyvinyl chloride columns with diameters of 35 mm and 58 mm, a glass container with a 98 mm circumference, and a metal rectangular prism measuring 12 mm by 100 mm. The gripper displayed a capability to safely grasp weights of 2.58 kg, 3.85 kg, 3.74 kg, and 3.23 kg for these respective objects. It's interesting that the gripper's maximal weight-bearing capacity is

dependent on both the form and element composition of the items. Nevertheless, the data imply that the produced gripping devices demonstrates outstanding competence in managing big weights.

III. CONCLUSIONS

In this research, a unique circular-shaped gripping device with flexible qualities analogous to a natural rubber strip was designed by producing a vacuum inner the gripping device. Findings from experiments validated that this gripping device demonstrated the potential to conform to items of varied geometries, encompassing bottles, boxes, cones, and plates, guaranteeing a smooth fit thanks to the adaptation of the sponges and the exterior membrane. Achieving a full enclosure with no any spaces augments the touched surface area and reduces the contact pressure. Consequently, this revolutionary gripping device exhibits the potential to firmly capture things without needing exact contact locations, a feature vital for finger-shaped grippers. Additionally, the research illustrates that a robotic arm equipped with this gripper can lift considerable weights. Manipulating the inner pressure of air of the gripping device directly impacted its encapsulating force; simultaneously, the gripper displayed the capacity to handle delicate goods like soft bread without producing deformation via controlled lowering of internal air pressure.

The aforementioned findings imply numerous possible directions for further investigation. Initially, it is recognized that the existing gripper design falls short in creating touch with the concave surfaces of objects owing to its inclination to compress by lowering its circumferential length. To properly interact with concave features, there is a requirement for a partial expansion of the gripper's length. This expansion will offer a more significant contact area with the object, a key aspect when handling fragile goods. Consequently, the search of a deformable structure capable of tolerating indentation offers itself as a formidable and promising route for future exploration.

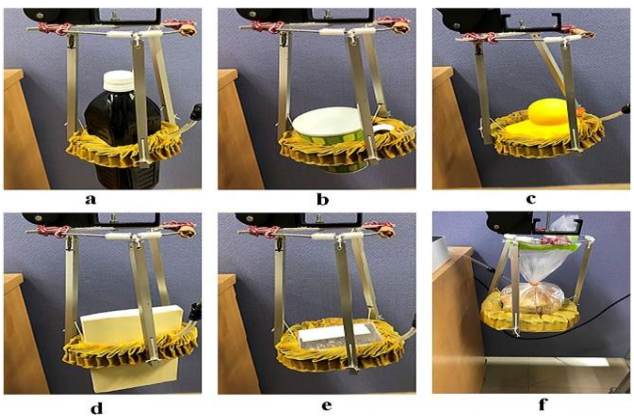

Figure 12: The Graspers Lift Assorted Items

In Figure 12, the graspers lift assorted items: a flask (900 g); b cup (280 g); c toy duck (65 g); d tome (165 g); e container (134 g); f a four-sided piece of bread (166 g). The grasper successfully hoisted objects of varying forms by enveloping them. In the case of the bread, the reduction of internal air pressure in the grasper was halted at – 3 kPa to prevent potential damage after securely enclosing the square loaf without any gaps.

The newly developed mounting device utilized malleable threads to make a connection between the connections and the gripping device. This technique permitted adjustable distortion of the gripping device, however it resulted in an unwanted swaying of the gripped item owing to the inherent freedom of movement in the links. This rocking motion must be reduced to accomplish accurate item placement. Furthermore, the existing connecting mechanism sets constraints on the gripper's usefulness, notably permitting it to handle things that are hung, since gravity naturally influences the gripper's capacity to place downward-hanging objects. If the gripping device could imitate the position of the automated arm, it would dramatically extend its possible uses.

Theoretical investigation of the gripper's deformation serves as a significant element. A complete research of the relationship between the sponge and outer membrane during gripper contraction is necessary. This experiment exhibits the gripper's power to wrap an item with a variable gradient. While the maximum limits of inclinations for cones have been addressed, this research remains unexplored for other geometric structures like triangular pyramids. Consequently, an appraisal of three-dimensional object wrapping is necessary.

CONFLICTS OF INTEREST

The authors declare that they have no conflicts of interest.

REFERENCES

[1] Trivedi D, Rahn CD, Kier WM, et al. (2008) Soft Robotics: Biological Inspiration, State of the Art, and Future Research. Appl Bionics Biomech. https://doi.org/10.1155/2008/530640

[2] Glick P, Hutchins E, Amador C, et al. (2018) Design and analysis of a soft robotic arm for dynamic manipulation. In: 2018 IEEE/RSJ International Conference on Intelligent Robots and Systems (IROS), Madrid, Spain. https://doi.org/10.1109/IROS.2018.8593788

[3] Yuk H, Lu B, Zhao X (2019) Hydrogel bioelectronics. Chem Soc Rev. https://doi.org/10.1039/C8CS00400G

[4] Li S, Vogt D, Rus D, et al. (2017) Fluid-driven origami-inspired artificial muscles. Proc Natl Acad Sci USA. https://doi.org/10.1073/pnas.1713450114

[5] Mosadegh B, Polygerinos P, Keplinger C, et al. (2014) Pneumatic networks for soft robotics that actuate rapidly. Adv Funct Mater. https://doi.org/10.1002/adfm.201303288

[6] Martinez RV, Branch JL, Fish CR, et al. (2013) Robotic tentacles with three- dimensional mobility based on

flexible elastomers. Adv Mater. https://doi.org/10.1002/adma.201303187
[7] Follmer S, Leithinger D, Olwal A, et al. (2018) inFORM: A Dynamic Shape Display for Interacting with Virtual and Physical 3D Objects. In: Proceedings of the 26th ACM Symposium on User Interface Software and Technology. https://doi.org/10.1145/2849243.2849275
[8] Bao G, Li X, Menciassi A (2015) Soft Robotics: Biological Inspiration, State of the Art, and Future Research. Appl Bionics Biomech. https://doi.org/10.1080/11762322.2015.1052687
[9] Kwiatkowski M, Ranzani T, Gerboni G, et al. (2017) Soft Robotic Grippers. In: Soft Robotics. Springer, Cham. https://doi.org/10.1007/978-3-319-41546-8_2
[10] Polygerinos P, Wang Z, Galloway KC, et al. (2015) Soft robotic glove for combined assistance and at-home rehabilitation. Robot Autonom Syst. https://doi.org/10.1016/j.robot.2015.01.003
[11] Calisti M, Picardi G, Levy G, et al. (2017) Octopus-Inspired Soft Robot: Pneumatically Actuated and Controlled Using an External Fluidic Reservoir. Bioinspir Biomim. https://doi.org/10.1088/1748-3190/aa5e17
[12] Connolly F, Walsh CJ, Bertoldi K (2015) Automatic Design of Fiber-Reinforced Soft Actuators for Shape-Changing Structures. PLoS ONE. https://doi.org/10.1371/journal.pone.0147942
[13] Tonazzini A, Sadeghi A, Cianchetti M, et al. (2015) Soft Robotic Manipulators as Tools for Neuroscience. In: Biomimetic and Biohybrid Systems. Springer, Cham. https://doi.org/10.1007/978-3-319-22979-9_22
[14] Xiao L, Hu W, Wu S, et al. (2020) A Soft Robotic Fish for Underwater Environmental Monitoring. In: 2020 IEEE/RSJ International Conference on Intelligent Robots and Systems (IROS), Las Vegas, NV, USA. https://doi.org/10.1109/IROS45743.2020.9340965
[15] Lu H, Yan J, Li H, et al. (2019) Development of a Novel Soft Robotic Fish with Multiple Undulating Fins for Bio-Inspired Underwater Propulsion. Front Robot AI. https://doi.org/10.3389/frobt.2019.00026
[16] Xiloyannis M, Tonazzini A, Sadeghi A, et al. (2016) A Soft Robotic Manipulator for Dexterous Interactions with Underwater Life. In: 2016 IEEE International Conference on Robotics and Automation (ICRA), Stockholm, Sweden. https://doi.org/10.1109/ICRA.2016.7487490
[17] Walker ID, Dawson DM, Priya S, et al. (2017) Soft Robotics for Neurorehabilitation. Soft Robot. https://doi.org/10.1089/soro.2017.0008
[18] Han L, Li Y, Zhang Z, et al. (2020) A Biomimetic Soft Robotic Fish Driven by Electroactive Polymer Actuators. IEEE Trans Ind Electron. https://doi.org/10.1109/TIE.2019.2892361
[19] Morin SA, Shepherd RF, Kwok SW, et al. (2012) Camouflage and Display for Soft Machines. Science. https://doi.org/10.1126/science.1222149
[20] Beccai L, Roccella S, Ascari L, et al. (2005) Design and Fabrication of a Soft Robotic Hand Able to Grasp and Identify Objects. Int J Robot Res. https://doi.org/10.1177/0278364905054810
[21] Chen A, Pei Q (2017) Making Robots with Thermoplastic Elastomers. Science Robotics. https://doi.org/10.1126/scirobotics.aao1893
[22] Kellaris N, Farrow N, Tolley MT (2019) Soft Robotic Quadrupedal Locomotion over Unconsolidated and Gap-Ridden Ground. Sci Robot. https://doi.org/10.1126/scirobotics.aaw3096